ELSEVIER

Chemometrics and Intelligent Laboratory Systems 50 (2000) 83–90

Chemometrics and intelligent laboratory systems

www.elsevier.com/locate/chemometrics

Optimal model-based experimental design in batch crystallization

Serena H. Chung, David L. Ma, Richard D. Braatz *

Department of Chemical Engineering, University of Illinois at Urbana-Champaign, 600 South Mathews Avenue, Box C-3, Urbana, IL 61801-3792, USA

Received 10 November 1998; accepted 3 August 1999

Abstract

The model-based experimental design of batch crystallizers is investigated. A dynamic programming formulation minimizes the volume of a confidence hyperellipsoid for the estimated nucleation and growth parameters over the supersaturation profile and the seed characteristics, namely, the crystal mass, mean size, and width of the seed distribution. It is shown that the accuracy of the parameter estimates can vary by several orders of magnitude depending on the seed characteristics, and that highly accurate estimation of nucleation and growth parameters can be obtained with as few as four batch experiments.

Keywords: Optimal experimental design; Crystallization

1. Introduction

Crystallization from solution is an industrially important unit operation due to its ability to provide high purity separations. The crystal size distribution (CSD) is a key factor in the production of high quality products and for determining the efficiency of downstream operations, such as filtration and washing. Batch crystallizers are widely used in industry, and a large proportion of these crystallizers are seeded.

The crystal growth and nucleation kinetic parameters must be determined experimentally before systematically designing a crystallizer and computing optimal operations and control procedures. The reliance on experiments to estimate these parameters arises due to an insufficient fundamental understanding of the nucleation and growth phenomena to derive the kinetics from first principles [1,2], and the strong sensitivity of most crystallizations to trace unmeasured chemical species in the feedstocks. The benefits of reducing the cost and time required to do experiments can be significant. For instance, in the pharmaceutical industries there is a huge pressure to bring a crystal product to market as fast as possible, since the first company to put a new product on the shelf usually captures the most of the market, even if a somewhat superior product is made available shortly thereafter. In such an environment, even a small reduction in the number of experiments can result in huge profitability increases.

In this paper, we apply model-based experimental design to a crystallization process in order to minimize the number of experiments required to construct a sufficiently accurate model. The accuracy of

* Corresponding author. Tel.: +1-217-333-5073; fax: +1-217-333-5052; e-mail: braatz@uiuc.edu

0169-7439/00/$ - see front matter
PII: S0169-7439(99)00049-0

the estimated parameters is quantified by a hyperellipsoid, whose size is a function of the informativeness of the data used in the parameter estimation procedure. The model-based design procedure computes experimental conditions that optimize the informativeness of the data, where the experimental design variables are the supersaturation profile and the seed characteristics.

This paper appears to be the most comprehensive study ever conducted on the model-based experimental design of a crystallization process. It is the first study to include seed characteristics as well as the supersaturation profile in the experimental design. It is shown that this allows highly accurate estimation of nucleation and growth parameters to be obtained with as few as four batch experiments. The software implementing the algorithms has been made available to the crystallization community via the web.

The paper is organized as follows. The process model and the dynamic programming formulation of the experimental design procedure are summarized first, then the method is applied to a simulated batch crystallizer. The final results are used to draw some important conclusions.

2. Batch crystallization model

It is assumed that all crystallization experiments are conducted in a batch crystallizer since this is significantly less time-consuming than experiments performed in other (e.g., MSMPR) crystallizers [3]. The batch crystallizer model is summarized briefly since excellent descriptions are given elsewhere [3,4].

Fig. 1 is the schematic diagram of a jacketed batch crystallizer. Water moving through the jacket is used to specify the temperature T in the crystallizer. Assume that the batch crystallizer has constant volume, is well-mixed, and that physical processes such as agglomeration, fracture, and attrition are negligible. Also assume that the crystals are characterized by one characteristic length L, with the constant volumetric shape factor k_v and surface area shape factor k_a. Then the population balance equation is [3,4]:

$$\frac{\partial f(L,t)}{\partial t} + \frac{\partial\{G(S,\boldsymbol{\theta}_g,L)f\}}{\partial L} = B(S,\boldsymbol{\theta}_b) \qquad (1)$$

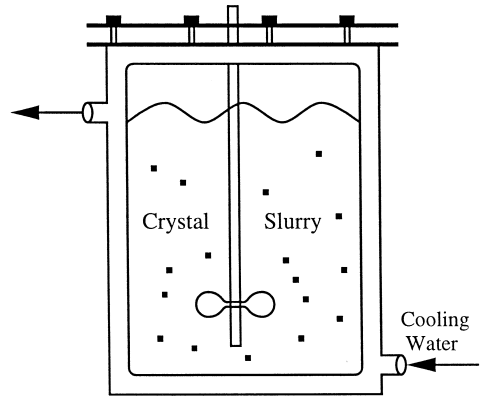

Fig. 1. A jacketed batch crystallizer.

where t is time, $f(L,t)$ is the number density function, $G(S,\boldsymbol{\theta}_g,L)$ is the crystal growth rate, $B(S,\boldsymbol{\theta}_b)$ is the nucleation rate, $S=(C-C_{sat})/C_{sat}$ is the relative supersaturation, C is the solute concentration, C_{sat} is the saturation concentration, and $\boldsymbol{\theta}_g$ and $\boldsymbol{\theta}_b$ are the growth and nucleation parameters, respectively.

Several models for growth rate have been developed depending on the crystals and crystallization processes [5–7]. The most popular model is given by [3]:

$$G = k_g S^g \qquad (2)$$

where k_g and g are the growth parameters.

In general nucleation is classified into two categories: primary or secondary [3]. This paper considers secondary nucleation from crystal surfaces, since it is the predominant mechanism taking place in most seeded batch crystallizers. The nucleation rate is assumed proportional to the collision energy, with the rest of the kinetics being in standard power law form [8]:

$$B = k_b S^b \hat{\mu}_3 \qquad (3)$$

where k_b and b are the nucleation parameters, and $\hat{\mu}_3$ is the third moment, as defined below.

The method of moments replaces the partial differential Eq. (1) by a set of ordinary differential equations, which simplifies the simulation of the batch crystallizer. The moment equations are derived

by multiplying Eq. (1) by L^j, integrating over L, and placing on a per mass of solvent basis [4]:

$$\frac{d\hat{\mu}_0}{dt} = B$$

$$\frac{d\hat{\mu}_j}{dt} = jG\hat{\mu}_{j-1} + Br_0^j \qquad j = 1,2,\ldots \tag{4}$$

where r_0 is crystal size at nucleation and is assumed to be a constant, and the j-th moment is defined by

$$\hat{\mu}_j \equiv \int_0^\infty L^j \hat{f}(L,t)\,dL \tag{5}$$

where $\hat{f}(L,T)$ is the population density function on a per mass of solvent basis.

The seed distribution, represented as shown in Fig. 2, is characterized by three parameters. The initial mass of seed crystals is m_{seed}, $\bar{L}_0$ is the mean size of the seed crystals, and W is the width of the seed distribution. Narrow seed distributions have W near 0, with $W = 1$ indicating a range of seed sizes from infinitesimal to twice the mean seed crystal size.

The amount of solute leaving the solution must be accounted by crystal growth and nucleation:

$$\frac{d\hat{C}}{dt} = -3\rho_c k_v G\hat{\mu}_2 - \rho_c k_v B r_0^3 \tag{6}$$

where ρ_c is density of the crystal and r_0 is the size of the crystal at nucleation.

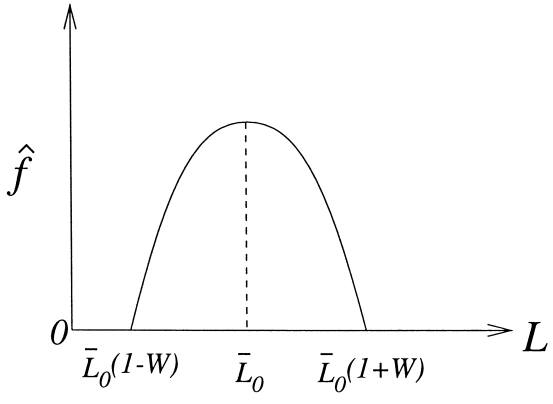

Fig. 2. Seed distribution: $\bar{L}_0 = \hat{\mu}_1 / \hat{\mu}_0$ is the mean size, $W \in [0,1]$ quantifies the width of the distribution.

3. Model-based experimental design

The model-based experimental design procedure is applied sequentially. Initial estimates of the parameters are used to compute the first experimental design, which is implemented in the laboratory. The data which are collected are used to compute improved parameter estimates and the associated confidence hyperellipsoid, which are both used in computing the experimental design for the next laboratory experiment. Since excellent descriptions of parameter estimation and model-based experimental design procedures are provided in textbooks [9,10], only a brief description is given here.

The parameter estimation problem is posed as a nonlinear optimization problem; here we use the objective

$$\Phi(\boldsymbol{\theta}) = \sum_{i=1}^{N_m} \sum_{j=1}^{N_d} w_{ij}\left(y_{ij} - \tilde{y}_{ij}\right)^2 \tag{7}$$

where $\boldsymbol{\theta}$ is the parameter vector, y_{ij} and $\tilde{y}_{ij}$ are the measurement and model prediction of the i-th measured variable at the j-th sampling instant, w_{ij} is a weighting factor, N_m is number of measured variables, and N_d is the number of sampling instances. To compute the maximum likelihood estimate of the parameters, each w_{ij} in Eq. (7) is set equal to the inverse of the measurement error variance [10].

Due to random errors associated with measurements, the parameter estimates are also random variables with probability distributions. An approximate confidence region for the parameters can be obtained by linearizing the model near the vicinity of the estimate [10]:

$$\tilde{\boldsymbol{y}}_j(\boldsymbol{\theta}) \approx \tilde{\boldsymbol{y}}_j(\boldsymbol{\theta}^*) + \mathbf{F}_j(\boldsymbol{\theta}^*)(\boldsymbol{\theta} - \boldsymbol{\theta}^*) \tag{8}$$

where $\tilde{\boldsymbol{y}}_j = [\tilde{\boldsymbol{y}}_{1j}, \ldots, \tilde{\boldsymbol{y}}_{N_{m,j}}]$ is the vector of model predictions at the j-th instant, $\boldsymbol{\theta}^*$ is the best estimate, and $\mathbf{F}_j$ is the $N_m \times N_p$ matrix given by

$$\mathbf{F}_j = \left.\frac{\partial \tilde{\mathbf{y}}_j}{\partial \boldsymbol{\theta}}\right|_{\boldsymbol{\theta}^*} \tag{9}$$

Although the matrices $\mathbf{F}_j$ can be calculated using finite differences, a more accurate way is to integrate the sensitivity equations along with the model equations [11].

For crystallization experiments it is normally acceptable to assume that the measurement errors are normally distributed and independent of each other, that is, the measurement error covariance matrix $\mathbf{V}$ is diagonal with the diagonal entries $\mathbf{V}_{ii} = \sigma_i^2$. Then the parameter covariance matrix $\mathbf{V}_\theta$ for the linearized problem is given by

$$\mathbf{V}_\theta^{-1} = \sum_{j=1}^{N_d} \mathbf{F}_j^T \mathbf{V}^{-1} \mathbf{F}_j.$$

The approximate $100(1-\alpha)\%$ confidence region is the hyperellipsoid defined by

$$(\boldsymbol{\theta} - \boldsymbol{\theta}^*)^T \mathbf{V}_\theta^{-1} (\boldsymbol{\theta} - \boldsymbol{\theta}^*) \le \chi^2_{N_p}(\alpha) \tag{10}$$

where χ^2 is the chi-squared distribution [10].

The eigenvectors of $\mathbf{V}_\theta^{-1}$ give the direction and the eigenvalues give the length of the axes of the hyperellipsoid. Because it is impossible to visualize a four-dimensional figure, confidence intervals are reported:

$$\boldsymbol{\theta}_i^* - \sqrt{\chi^2_{N_p}(\alpha)\mathbf{V}_{\theta,ii}} \le \boldsymbol{\theta}_i \le \boldsymbol{\theta}_i^* + \sqrt{\chi^2_{N_p}(\alpha)\mathbf{V}_{\theta,ii}} \tag{11}$$

where $\mathbf{V}_{\theta,ii}$ is the (i,i) element of $\mathbf{V}_\theta$.

The model-based optimal experimental design procedure computes experimental conditions that minimize the uncertainty in the estimated parameters, which is quantified by the volume of the confidence hyperellipsoid (this is called D-optimality [9]). The volume of the hyperellipsoid (Eq. (10)) is inversely proportional to the determinant of $\mathbf{V}_\theta^{-1}$, hence to minimize the volume is to maximize the objective function

$$\psi\left(\mathbf{u}(t); \hat{\boldsymbol{\theta}}\right) = |\mathbf{V}_\theta^{-1}| = \left| \sum_{j=1}^{N_d} \mathbf{F}_j^T \mathbf{V}^{-1} \mathbf{F}_j \right|. \tag{12}$$

For specificity, we consider the case where the supersaturation is created by reducing the temperature $T(t)$, although other methods of achieving supersaturation such as antisolvent addition [12] can be formulated in a similar manner. The dynamic programming formulation is generalization of [13]:

$$\begin{aligned}
\max_{T(t), m_{seed}, \bar{L}_0, W} \quad & \psi \\
\text{subject to} \quad & g_1(t) = T_{min} - T(t) \le 0 \\
& g_2(t) = T(t) - T_{max} \le 0 \\
& g_3(t) = \frac{dT(t)}{dt} - R_{max} \le 0 \\
& g_4(t) = R_{min} - \frac{dT(t)}{dt} \le 0 \\
& g_5 = m_{seed,min} - m_{seed} \le 0 \\
& g_6 = m_{seed} - m_{seed,max} \le 0 \\
& g_7 = \bar{L}_{0,min} - \bar{L}_0 \le 0 \\
& g_8 = \bar{L}_0 - \bar{L}_{0,max} \le 0 \\
& g_9 = W_{min} - W \le 0 \\
& g_{10} = W - W_{max} \le 0
\end{aligned} \tag{13}$$

The temperature constraints $g_1(t)$ to $g_4(t)$ ensure that the temperature profile stays within the operating range of the crystallizer. The constraints g_5 to g_{10} ensure that the seed distribution is practical. For example, for economic reasons the seed mass is usually constrained to be less than 10% of the final crystal mass.

4. Results

The measurements selected for this study are concentration and transmittance ($N_m = 2$). Transmittance is related to the second moment by

$$\text{transmittance} = I = \exp\left(-\frac{k_a}{2} \frac{m_{solvent}}{m_{slurry}} l \hat{\mu}_2 \right) \tag{14}$$

where l is the cell length, $m_{solvent}$ is mass of the solvent, and m_{slurry} is mass of the slurry. Therefore, at the j-th sampling time the measurements are

$$\mathbf{y}_j = \begin{bmatrix} I_j \\ \hat{C}_j \end{bmatrix}. \tag{15}$$

Each measurement is assumed to have additive normally distributed noise with variances σ_I^2 and σ_C^2,

Table 1
Parameters used in the simulation study

Variable	Name	Value	Units
m_{solvent}	mass of solvent	7.57×10^6	g
$\rho_c^{\dagger}$	density of crystal	2.11	g/cm^3
$r_0^{\dagger}$	nucleated crystal size	0	μm
$\hat{C}$	solute concentration		g KNO_3/g H_2O
$\hat{C}_{\text{sat}}^{\dagger}$	saturation concentration	$0.1286 + 0.00588T + 0.0001721T^2$	g KNO_3/g H_2O
$k_a^{\dagger}$	surface area shape factor	6	dimensionless
$k_v^{\dagger}$	volumetric shape factor	1	dimensionless
$k_b^{\dagger}$	nucleation parameter	exp(17.142)	#/cm^3 min
$b^{\dagger}$	nucleation parameter	1.78	dimensionless
$k_g^{\dagger}$	growth parameter	exp(8.849)	μm/min
$g^{\dagger}$	growth parameter	1.32	dimensionless
$l^{\dagger}$	cell length	1.77	mm
T	crystallizer temperature		°C
$T_{\max}$	maximum T constraint	32.3	°C
$T_{\min}$	minimum T constraint	22.0	°C
$R_{\max}$	maximum rate of T change	0.0	°C/min
$R_{\min}$	minimum rate of T change	-0.1	°C/min
$m_{\text{seed,max}}$	maximum seed mass	110,000	g
$m_{\text{seed,min}}$	minimum seed mass	5.0	g
$\bar{L}_{0,\max}$	maximum mean seed size	600	μm
$\bar{L}_{0,\min}$	minimum mean seed size	5.0	μm
$W_{\max}$	maximum percent width of seed distribution	0.95	dimensionless
$W_{\min}$	minimum percent width of seed distribution	0.05	dimensionless
$\sigma_I^{2\dagger}$	variance of transmittance measurement	$(0.009)^2$	dimensionless
$\sigma_C^{2\dagger}$	variance of concentration measurement	$(0.0005)^2$	(g KNO_3/g H_2O)^2
N_d	number of sampling instances	160	dimensionless
Δt	sampling time	1.0	min

†Parameters are from Miller [14].

Table 2
Estimated parameters and 95% confidence intervals for different experimental designs. The true parameter values are given in Table 1. MBED stands for ''model-based experimental design''

Number of data sets		Sequential MBED	Natural cooling	Linear cooling
1	g	1.289 ± 0.071	1.316 ± 0.102	1.315 ± 0.095
	$\ln k_g$	8.749 ± 0.242	8.829 ± 0.468	8.835 ± 0.413
	b	1.752 ± 0.140	2.402 ± 1.179	1.776 ± 0.285
	$\ln k_b$	17.048 ± 0.492	19.796 ± 5.344	17.137 ± 1.291
2	g	1.321 ± 0.025	1.375 ± 0.103	1.313 ± 0.080
	$\ln k_g$	8.849 ± 0.094	9.093 ± 0.475	8.825 ± 0.343
	b	1.784 ± 0.046	1.723 ± 0.568	1.770 ± 0.240
	$\ln k_b$	17.154 ± 0.191	16.882 ± 2.643	17.106 ± 1.079
3	g	1.323 ± 0.027	1.325 ± 0.102	1.291 ± 0.072
	$\ln k_g$	8.860 ± 0.097	8.870 ± 0.471	8.731 ± 0.308
	b	1.781 ± 0.074	1.595 ± 0.528	1.747 ± 0.213
	$\ln k_b$	17.136 ± 0.266	16.287 ± 2.473	17.005 ± 0.954
4	g	1.317 ± 0.019	1.350 ± 0.103	1.299 ± 0.065
	$\ln k_g$	8.838 ± 0.070	8.989 ± 0.473	8.762 ± 0.280
	b	1.781 ± 0.035	1.652 ± 0.541	1.786 ± 0.205
	$\ln k_b$	17.136 ± 0.137	16.588 ± 2.529	17.180 ± 0.911

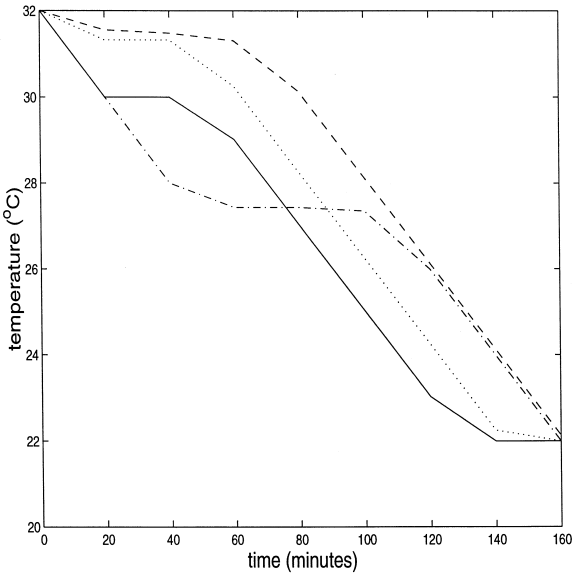

Fig. 3. Temperature profile for optimal experimental design: step 1 (—), step 2 (---), step 3 (- · -), and step 4 (· · ·).

respectively. The parameters to be estimated are $\boldsymbol{\theta}^{\mathrm{T}} = [g, k_g, b, k_b]$ defined in Eqs. (2) and (3).

Table 1 lists the properties of the KNO_3–H_2O batch cooling crystallizer used in this study. All variables are defined in Sections 2–4. The nucleation and growth parameters $b^{\dagger}$, $k_b^{\dagger}$, $g^{\dagger}$, $k_g^{\dagger}$ were obtained through a thorough experimental study [14], and these are treated as the true values for this study. The moment equations were integrated for a production run of 160 min using Gear's stiff method [15]. The cooling profile $T(t)$ was parameterized by a linear spline [16] to reduce the infinite dimensional nonlinear program to a finite dimensional nonlinear program, which was solved using successive quadratic programming [17]. The software implementing the algorithms has been made available to the crystallization community via the web [18].

For sequential optimal model-based experimental design, the initial design is based on setting the kinetic parameters equal to the midpoint of the range of possible values as given in [3] ($g = 1.5$, $\ln k_g = 5$, $b = 2$, and $\ln k_b = 10$). The obtained experimental data are then used to improve the parameter estimates, and to design the next experiment. The procedure was repeated until the relative error in each kinetic parameter was less than 2%. Each set of parameter estimates is listed in Table 2 with estimates obtained by linear and natural cooling. The obtained temperature profile and the seed distribution for the model-based experimental design are given in Fig. 3 and Table 3, respectively.

Table 2 shows that the parameter estimates obtained by the model-based design procedure for a single experimental run are more accurate than for four experimental runs using natural cooling or linear cooling. Comparing the designs where four experimental runs are used, the parameter estimates obtained by the model-based experimental design procedure are approximately an order of magnitude more accurate than for the other designs. Better parameter estimates were obtained by linear cooling than natural cooling.

Fig. 3 and Table 3 indicate that the supersaturation profile and the mean seed size for the optimal experimental design can change substantially from one iteration to the next. For each experiment, the temperature profile is at its maximum or minimum rate constraint during most of the run. The maximum rate constraint can occur at the beginning, middle, and/or end of the run. As shown in Table 3, the seed mass is small for all optimal experimental designs. Reducing the amount of initial seed causes the supersaturation to be larger throughout the experiment, providing better signal-to-noise ratios for determining parameter values (see Eqs. (2) and (3)). This is in sharp contrast to which seed characteristics are desirable for optimal control of product crystal properties [19] in which large seed masses are used to promote growth over nucleation.

Recall from Section 3 that $|\mathbf{V}_{\theta}^{-1}|$ is inversely proportional to the volume of the hyperellipsoid defin-

Table 3
Optimal seed distribution for sequential optimal experiment designs. A seed distribution similar to Miller's [14] was used for the linear and natural cooling profiles

	m_{seed} (g)	$\bar{L}_0$ (μm)	W
Miller's	230	196	0.612
MBED steps 1–3	5.0	600	0.95
MBED step 4	5.0	142	0.95

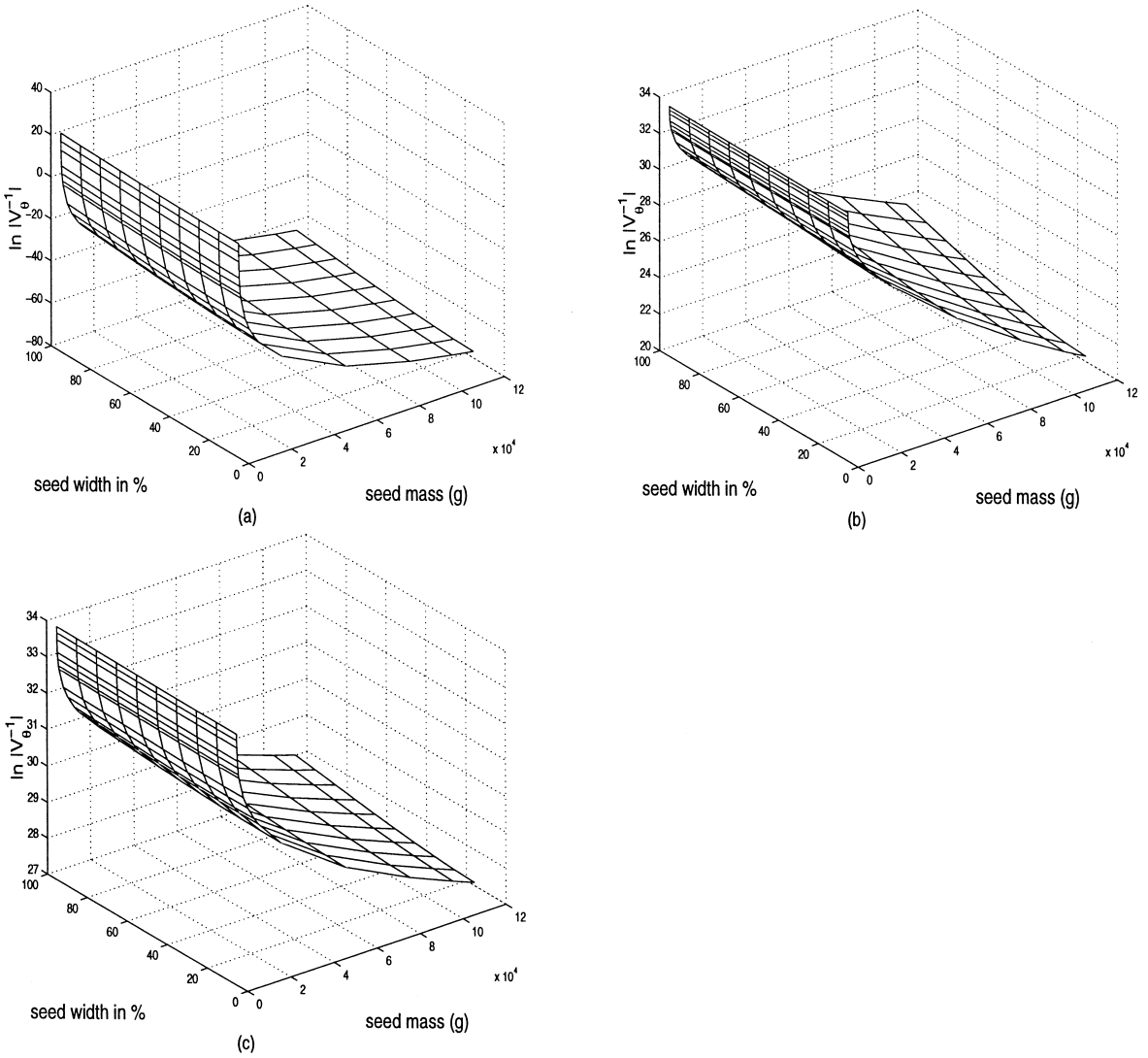

Fig. 4. Plot of ln $|\mathbf{V}_\theta^{-1}|$ vs. seed mass and percent width: (a) at mean seed size $\bar{L}_0 = 10$ μm; (b) $\bar{L}_0 = 250$ μm; (c) $\bar{L}_0 = 550$ μm.

ing the confidence region for the model parameters. In other words, $|\mathbf{V}_\theta^{-1}|$ quantifies the informativeness the experimental data — the larger its value, the more informative the data, and the more accurate the resulting parameter estimates. To determine the magnitude of the effect of the seed distribution on the informativeness the experimental data, ln $|\mathbf{V}_\theta^{-1}|$ was plotted for the range of seed distributions for a fixed temperature profile in Fig. 4. It shows that the accuracy of the parameter estimates can vary by several orders of magnitude depending on the seed characteristics, the most important being the seed mass and mean size. As seen in Table 3, a small seed mass gives the most informative experimental data.

Before this work, the most sophisticated study of the model-based experimental design of crystallization processes appears to be that of Matthews [13]. The main differences between our study and that of Matthews [13] are that our study: (1) considers a much wider range of seed masses, (2) starts from relatively low accuracy parameter estimates as would be expected in practice, (3) optimizes over the seed distribution, which can have orders-of-magnitude effect on the accuracy of the estimated parameters, and (4) compares sequential model-based experimental design to the standard alternatives (Table 3).

5. Conclusions

The crystallization study can be used to draw some general conclusions. Highly accurate estimation of nucleation and growth parameters can be obtained with as few as four batch experiments. The seed characteristics have a much stronger effect on the quality of the parameter estimates than minor modifications of the supersaturation profile. Small seed masses should be used when collecting experimental data.

To encourage the application of optimal model-based experimental design to industrial crystallization, the algorithms used in this study have been made available via the web [18].

Acknowledgements

S.H. Chung acknowledges the support of the Hauser scholarship. David L. Ma and R.D. Braatz acknowledge the support of Merck and the National Center for Supercomputing Applications.

References

[1] J.W. Mullin, Crystallization, 2nd edn., CRC Press, Cleveland, OH, 1972.
[2] D.W. Oxtoby, Homogeneous nucleation: theory and experiment, J. Phys. Condens. Matter 4 (1992) 7627–7650.
[3] A. Randolph, M.A. Larson, Theory of Particulate Processes, 2nd edn., Academic Press, San Diego, 1988.
[4] H.M. Hulburt, S. Katz, Some problems in particle technology, Chem. Eng. Sci. 19 (1964) 555–574.
[5] J. Garside, Advances in characterisation of crystal growth, in: Advances in Crystallization from Solutions, AIChE Symp. Ser. 80 (240) (1984) 23–38, AIChE, New York.
[6] M. O'Hara, R.C. Reid, Modelling Crystal Growth Rates from Solution, Prentice-Hall, Englewood Cliffs, NJ, 1973.
[7] W. Burton, N. Cabrera, F. Frank, The growth of crystals and the equilibrium structure of their surfaces, Philos. Trans. R. Soc. London, Ser. B 243 (1951) 299–358.
[8] J. Nyvlt, O. Sohnel, M. Matuchova, M. Broul, The kinetics of industrial crystallization, Chem. Eng. Monogr. 19 (1985) .
[9] A.C. Atkinson, A.N. Donev, Optimum Experimental Designs, Oxford Univ. Press, New York, 1992.
[10] J.V. Beck, K.J. Arnold, Parameter Estimation in Engineering and Science, Wiley, New York, 1977.
[11] M. Caracotsios, W.E. Stewart, Sensitivity analysis of initial value problems with mixed ODEs and algebraic equations, Comput. Chem. Eng. 9 (1985) 359–365.
[12] H. Charmolue, R.W. Rousseau, L-Serine obtained by methanol addition in batch crystallization, AIChE J. 37 (1991) 1121–1128.
[13] H.B. Matthews III, Model identification and control of batch crystallization for an industrial chemical system, PhD Thesis, University of Wisconsin, Madison, 1997.
[14] S.M. Miller, Modelling and quality control strategies for batch cooling crystallizers, PhD Thesis, Univ. of Texas at Austin, 1993.
[15] IMSL, Visual Numerics, 1997 (computer software).
[16] C.R. Wylie, L.C. Barrett, Advanced Engineering Mathematics, 6th edn., McGraw-Hill, New York, 1995.
[17] J.L. Zhou, A.L. Tits, C.T. Lawrence, FFSQP, University of Maryland, College Park, 1989, http://www.isr.umd.edu/labs/cacse/fsqp/fsqp.html (computer software).
[18] S.H. Chung, D.L. Ma, R.D. Braatz, FORTRAN Software for Simulation, Parameter Estimation, Experimental Design, and Optimal Control of Crystal Growth, University of Illinois, Urbana, 1999, http://brahms.scs.uiuc.edu/ ~ erp/lssrl/software/crystal (computer software).
[19] B.K. Johnson, C. Szeto, O. Davidson, A. Andrews, Optimization of pharmaceutical batch crystallization for filtration and scale-up, AIChE Annu. Meet. (1997).